Staged control of domestic hot water storage tanks to support district heating efficiency

Tahiri, Abdelkarim; Smith, Kevin Michael; Thorsen, Jan Eric; Hviid, Christian Anker; Svendsen, Svend

Published in:
Energy

Link to article, DOI:
10.1016/j.energy.2022.125493

Publication date:
2023

Document Version
Publisher's PDF, also known as Version of record

Energy 263 (2023) 125493

Contents lists available at ScienceDirect

Energy

journal homepage: www.elsevier.com/locate/energy

Staged control of domestic hot water storage tanks to support district heating efficiency

Abdelkarim Tahiri [a,*], Kevin Michael Smith [a], Jan Eric Thorsen [b], Christian Anker Hviid [a], Svend Svendsen [a]

[a] Section for Energy and Services, Department of Civil and Mechanical Engineering, Technical University of Denmark, Kgs. Lyngby, 2800, Denmark
[b] Danfoss Climate Solutions, Nordborg, Denmark

ARTICLE INFO

Keywords:
Domestic hot water tank
Control strategy
Modelica model
District heating
Return temperature

ABSTRACT

Storage tanks are commonly used for domestic hot water (DHW) preparation in large buildings supplied by district heating (DH), especially to cope with peak demand. The charging control of DHW tank systems is often suboptimal, increasing return temperatures and harming the overall DH operation efficiency. This paper presents two novel control concepts to optimize DHW tank charging, satisfying comfort and hygienic requirements without leading to excessive DH flows. The first, more complex control concept employs the smart energy meter sometimes used for DHW billing. It inspired the development of a second, broadly implementable control concept employing a staged proportional gain with an added temperature sensor. The authors tested and refined this staged-gain concept using a validated Modelica model of a real DHW system in a Danish multistory residential building. The authors subsequently implemented the staged-gain control concept in the field, successfully reducing the energy-weighted DH return temperature by 7 °C and the total DH flow by 23.6% compared to the conventional thermostatic control. This analysis accounted for the variation in DHW tapping, DHW temperature, DH supply temperature, and cold water temperature. Furthermore, the performance was robust to relaxed settings of the valve constraints, demonstrating minimal configuration requirements for new implementations.

1. Introduction

In the race for energy system decarbonization, EU policies aim to cut greenhouse gas emissions by 55% by 2030 compared to 1990 levels [1]. This target will reshape energy production and consumption in different sectors of society. Among cold climate countries, the widespread use of district heating (DH) networks is essential in the transition to an emission-free building heating system, thus enabling the integration of large amounts of renewable energy and excess heat into the grid [2–4]. Specifically, low-temperature district heating (LTDH) systems, with supply and return temperatures about 55 °C and 25 °C, respectively, offer a cost-effective DH operation to lead the shift to a fossil-free energy system [2–4]. In certain European countries, e.g. Denmark and Latvia, more than 60% of the citizens are connected to DH [5], which typically supplies energy to the space heating (SH) and domestic hot water (DHW) systems. In particular, the estimated energy used for DHW preparation accounts for 16% to 50% of total heating demand in European households [6]. This share has increased significantly over the years and is expected to be dominant in the future due to increasingly strict standards for new buildings [7,8]. Ivanko et al. [9] underscored the importance of reducing heat use for DHW production as the critical component for energy savings, especially in passive houses and well-insulated buildings. The share of DH used for DHW preparation can be as high as 45–50% in new or energy-renovated multi-family buildings [10].

Suitable operating temperatures for DHW systems depend on the type of installation. A storage tank with internal heating coil and circulation loop is widely used in the Greater Copenhagen area. The DHW supply temperature must comply with comfort and hygiene requirements. According to the Danish standards [11,12], DHW systems with temperature sterilization, must secure at least 50 °C in the circulation loop to avoid the growth of Legionella. Only situations with extraordinary tapping permit down to 45 °C. Thus, the system operators usually set the DHW supply temperature to 55 °C to compensate for circulation heat losses.

Several obstacles can harm the operation of DHW systems. In many buildings, the heat for circulation constitutes a high percentage of the total demand for DHW preparation, resulting in high return temperatures [13]. The return temperature of the circulation flow is 50 °C,

* Corresponding author.
E-mail address: abta@byg.dtu.dk (A. Tahiri).

https://doi.org/10.1016/j.energy.2022.125493
Received 26 April 2022; Received in revised form 30 August 2022; Accepted 17 September 2022
Available online 22 September 2022

Nomenclature

Acronyms

DHW	Domestic Hot Water
DH	District Heating
LTDH	Low-Temperature District Heating
SH	Space Heating
ULTDH	Ultra Low-Temperature District Heating
VP	Valve Position

Subscripts

circ	Circulation
cw	Cold Water
high	High level
ins	Instant
threshold	Preset threshold
low	Low level
max	Maximum
medium	Medium level
ret	Return
set	Set-point
sup	Supply

Symbols

Δ	Difference [-]
$\dot{m}$	Mass flow [kg/s]
c_w	Specific heat capacity of water [kJ/(kg °C)]
E	Energy [kWh]
P-band	Proportional band [°C]
P	Power [kW]
T	Temperature [°C]
UA	Heat transfer coefficient [kW/K]

and the circulation heat losses are constant, requiring a constant DH flow. This constrains the minimum return temperatures from buildings with high shares of circulation heat losses. Bøhm [7] documented the efficiency of DHW distribution systems in Danish apartment buildings and found that circulation heat losses ranged from 23% to 70% of the total heat used by the DHW installations. Likewise, the DHW consumption profile is another matter of concern. Occupants in residential buildings rarely consume hot water at night, yet the constant circulation heat losses demand constant DH flows. Since there is no cold-water entering the bottom part of the tank, the cooling of the DH flow is insufficient [13]. Several studies [6,14,15] have characterized the DHW consumption profile in an attempt to predict the demand pattern. Fuentes et al. [16] pointed out that further characterization of DHW demand will allow the design of novel control strategies based on consumption patterns. Another long-standing problem is excessive primary-side flow when heating the tank after a peak tapping of DHW. Here, the primary side describes the DH network, while the secondary side represents the building systems. For example, overdimensioned tank-charging flows can lead to relatively high peak DH demand immediately after the morning tapping of DHW. Averfalk et al. [17] focused on the primary side components of substations, which often deliver excessive flows due to oversized valves and heat exchangers. Measurements in a Swedish building revealed an overestimated simultaneity of DHW tapping, known as the coincidence factor, leading to excessive design flows. Yang et al. [18] evaluated the capacity of a DHW tank and confirmed the importance of properly sizing the control valve.

Multiple efforts have introduced hardware solutions to reduce return temperatures from DHW with high return temperatures due to relatively high circulation heat losses. Thorsen et al. [19] developed an alternative solution based on a booster heat pump to compensate for circulation heat losses. They successfully reduced the return temperature from 47 °C to 22 °C in a building where the circulation heat loss accounted for 70% of the total energy used for DHW consumption and circulation. Other solutions based on electrical boosting solutions in combination with ultra low-temperature district heating (ULTDH) systems have been studied [20], and other authors implemented a model predictive control algorithm to minimize the operation costs of such alternatives [21]. A considerable amount of research has suggested actions to lower return temperatures in DHW systems, but little research has focused on providing alternatives that do not incur additional investment.

Several studies have aimed to improve the charging control of DHW tanks. Yang and Honoré [22] introduced a heating capacity limitation for a DHW tank in a new building in Copenhagen and reduced the peak load from 70–80 kW to 25 kW. Huang et al. [23] developed and simulated a novel control method that similarly limited heating capacities but added a safety mode to allow higher heating capacities during periods with considerable DHW use. Yang et al. [24] proposed a new control strategy for charging DHW tanks and reduced the simulated DH return temperature and volume flow by 4.9–16.4 °C and 8–28%, respectively, compared to a reference case.

Prior investigations have indicated the preliminary potential of improved DHW tank charging for reducing DH return temperature and peak loads. Furthering this work, this study presents two new control concepts for DHW tank charging with a focus on maximizing applicability while minimizing DH return temperatures. The first proposal relies on smart energy meters, while the second strategy relies on a staged proportional controller with low complexity and straightforward implementation. The study evaluated the control concepts using detailed dynamic models, and the authors subsequently implemented the promising staged control concept in Hillerød, Denmark. The field tests comprehensively compared the performance of the new staged control concept with the conventional thermostatic control. To conduct a fair comparison, the study accounted for the relative circulation heat loss, the DHW supply temperature, the DH supply temperature, and the cold water temperature. Finally, the authors analyzed the operation of the control valve and the sensitivity of the controller's performance to its shaping parameters.

This manuscript includes the definition of the new control algorithms, an outline of the system, the modeling approach, the results from the tank model validation, the simulations of both strategies, and the field tests with the new staged control.

2. Methods

2.1. New control logic

Conventionally, a thermostat regulates the DH flow through the heating coil, often employing a proportional–integral controller, to maintain a set-point temperature at the location of the sensor in the tank. The new solution intends to prevent tank overcharging, i.e. to minimize situations with excessive heat input from the primary side.

This section introduces two new charging strategies to optimize DH supply. The first strategy uses data from the energy meters, usually installed for billing purposes. The aim is to constantly miminize heating of the tank to only what is necessary for circulation and DHW use. If successful, the tank's volume below the circulation remains cold as long as possible and enhances the tank's temperature gradient ahead of periods with low tapping. The second algorithm seeks to implement the same principle but without the need for the energy meter data, thereby maximizing applicability.

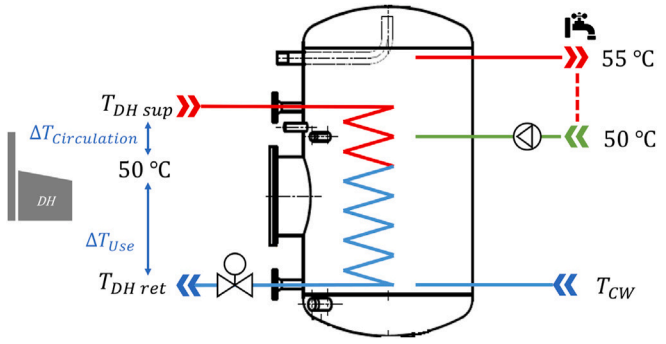

Fig. 1. Storage tank with an internal heating coil and a circulation loop supplied by district heating.

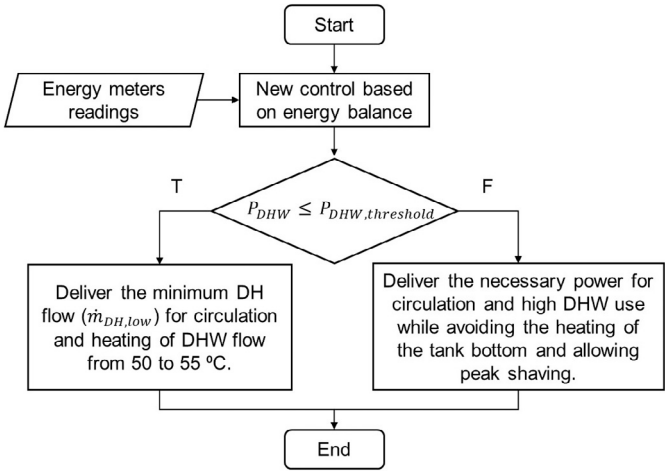

Fig. 2. Control logic for the new control strategy based on energy balance.

2.1.1. New charging strategy based on energy balance

Fig. 1 shows a schematic of the considered storage tank and the assumption that all heating from 50 to 55 °C cools the DH flow from its supply temperature ($T_{DH,sup}$) to 50 °C. The DH flow subsequently heats the cold water entering the tank bottom at T_{cw}. It is important to make this distinction because only the DH flow above 50 °C can heat the circulation. Based on these assumptions, the energy balance inside the tank can be characterized by Eq. (1),

$$\int_a^b P_{DH}\,dt = \int_a^b P_{circ}\,dt + \int_a^b P_{DHW}\,dt \tag{1}$$

where, P_{DH}, P_{circ} and P_{DHW} are the DH heat supplied to the tank [kW], the circulation losses [kW], and the heat consumption of DHW [kW], respectively. The energy loss through the tank walls is negligible compared to the aforementioned energy balance terms.

Energy meters, each comprising a flow meter and two temperature sensors, make up the metering system installed in the DHW substation. On the primary side, the meter determines the accumulated DH heat supplied to the tank by measuring the DH flow rate and the supply and return temperatures. The secondary side system meters the heating of tapped DHW by measuring the flow and temperature of the cold water intake and the temperature of the tapped DHW. The energy meters collect the necessary data for the calculation of P_{DH}, P_{circ} and P_{DHW}, enabling the application of the new control method. According to Eq. (1), the circulation heat losses are the difference between the heat supplied to the tank and the heat used to heat up the tapped DHW.

Fig. 2 outlines the new control concept. The algorithm reads the energy meters and, depending on whether the power for DHW use (P_{DHW}) is above or below a preset threshold ($P_{DHW,threshold}$), determines whether to deliver the necessary heating power for circulation and high DHW use or deliver the minimum flow for circulation and heating of DHW from 50 to 55 °C.

Different situations may occur throughout the day in terms of DHW consumption. The following four states describe the phenomena created in the tank, from lowest to highest tapping. These states give rise to the equations used by the algorithm and characterize the threshold ($P_{DHW,threshold}$) applied in the decision block of Fig. 2, which activates the corresponding charging mode.

State 1: Periods with no use of DHW ($P_{DHW} = 0$). When there is virtually no DHW demand, e.g. during the night, the DH flow still supplies continuous heating to cover the circulation losses. Consequently, the lower part of the coil heats the lower part of the tank. To start periods with no DHW demand, having cold water in the lower part of the tank helps to minimize the return temperatures. The primary flow $\dot{m}_{DH,circ}$ [kg/s] required to deliver the circulation heat loss can be calculated by Eq. (2),

$$\dot{m}_{DH,circ} = \frac{P_{circ}}{c_w \cdot (T_{DH,sup} - 50)} \tag{2}$$

where c_w represents the specific heat capacity of water (4.18 kJ/(kg °C)).

State 2: Periods with DHW use below the threshold ($P_{DHW} < P_{DHW,threshold}$). When there is low DHW consumption, a small DH flow $\dot{m}_{DH,low}$ covers both the heating of DHW flow from 50 to 55 °C ($P_{DHW,50-55}$) and the circulation heat loss. Compared to State 1, the primary flow $\dot{m}_{DH,low}$ is slightly larger, according to Eq. (3).

$$\dot{m}_{DH,low} = \frac{P_{circ} + P_{DHW,50-55}}{c_w \cdot (T_{DH,sup} - 50)} \tag{3}$$

where $P_{DHW,50-55}$ [kW] can be expressed by using a proportional temperature ratio, as shown in Eq. (4).

$$P_{DHW,50-55} = P_{DHW} \cdot \frac{55 - 50}{55 - T_{cw}} \tag{4}$$

State 3: Periods with DHW use corresponding to the threshold ($P_{DHW} = P_{DHW,threshold}$). In this situation, the coil supplies the exact amount of heating for DHW production and circulation. Therefore, there is no heating of the tank bottom or accumulation of heat (E_{stored}) due to the cooling of the DH flow from 50 °C to $T_{DH,ret}$. Conversely, during States 1 and 2, the supplied heat from the primary side is not immediately utilized on the secondary side for DHW production and circulation, as the DHW use is lower than the threshold. Consequently, stored heat (E_{stored}) remains in the tank as shown in Eq. (5).

$$E_{stored} = \int_0^\tau (P_{DH} - P_{circ} - P_{DHW})\,dt \tag{5}$$

The power needed for heating the DHW flow from T_{cw} to 50 °C in State 3 can be expressed as shown in the first term of Eq. (6).

$$P_{DHW,threshold} \cdot \frac{50 - T_{cw}}{55 - T_{cw}} = \dot{m}_{DH} \cdot c_w \cdot (50 - T_{DH,ret}) \tag{6}$$

The $P_{DHW,threshold}$ can be deduced from the relation in Eq. (7) by simplifying Eq. (6) and using expressions Eq. (3) and Eq. (4) with the DHW demand equal to the threshold.

$$P_{DHW,threshold} = \frac{P_{circ} \cdot (55 - T_{cw}) \cdot r}{(T_{DH,sup} - 50) + r \cdot (50 - 55)} \qquad where \quad r = \frac{50 - T_{DH,ret}}{50 - T_{cw}} \tag{7}$$

In the ideal event that $T_{DH,ret}$ equaled T_{cw}, one could simplify the equation by setting $r = 1$. However, this optimistic assumption is not considered here.

State 4: Periods with DHW use above the threshold ($P_{DHW} > P_{DHW,threshold}$). In States 1 and 2, the return temperature increases over time due to the heating of the tank bottom. To avoid this detrimental

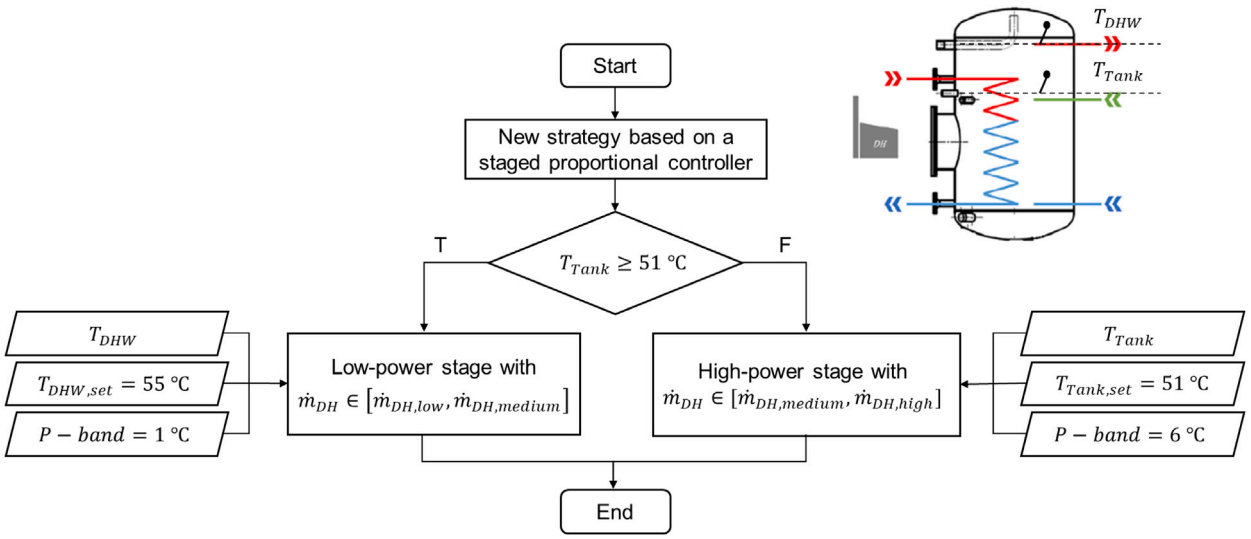

Fig. 3. Control logic for the new control strategy based on a staged proportional controller.

impact, the power supplied by the heating coil shall be regulated according to Eq. (8) when the use of DHW is higher than the threshold. The function f constitutes the utilized fraction of the stored heat. In this way, the utilization of this heat will shave the peak load in the morning, supplying only the strictly necessary DH flow.

$$P_{DH} = P_{circ} + P_{DHW} - f(E_{stored}) \tag{8}$$

The algorithm delivers the stored heat as early as possible during the first peaks in the morning, and all should be dispensed by the end of the day. In this sense, a precondition of this strategy is to have a sufficiently cold water tank at the beginning of those periods with hardly any DHW demand.

2.1.2. New charging strategy based on a staged proportional controller

The conventional thermostatic controller uses a temperature sensor well below the top of the tank (in layer 14 out of 40) to react early and avoid sudden temperature drops during periods with high tapping. In a simple proportional controller, the proportional band ($P - band$) determines the difference between the set-point and measured temperatures corresponding to a fully open valve with maximum DH flow. Fig. 3 describes the new control strategy consisting of a proportional controller with two proportional bands. At the very top of the tank (layer 1 of 40), an added temperature sensor measures the DHW supply temperature. This algorithm employs the sensors at layers 1 (T_{DHW}) and 14 (T_{Tank}) with corresponding set-points and, depending on whether the temperature at layer 14 is above or below 51 °C, determines whether to operate in a low-power stage or a high-power stage, respectively. In the low-power stage, the valve opens to a lesser extent, solely to compensate for circulation heat losses and the low demand that may exist for hot water. The control adjusts the set-point for the DHW supply temperature (T_{DHW}) to 55 °C with a P-band of 1 degree, thereby compensating for circulation heat losses at times of low consumption. Conversely, when the sensor at layer 14 measures a temperature below 51 °C due to high tapping, the controller switches to a high-power stage while supplying the necessary DH flow to avoid compromising hygiene and comfort conditions. In this case the set-point is 51 °C for T_{Tank} with a P-band of 6 °C, thus delivering the maximum DH flow when the sensor T_{Tank} reads the critical temperature of 45 °C.

Assuming a temperature difference of 1.5 °C between layers 1 (T_{DHW}) and 14 (T_{Tank}), Fig. 4 shows the primary flow corresponding to the measured temperature at T_{Tank}. Hence, at times with DHW supply temperature between 55 and 54 °C, the primary flow will range from $\dot{m}_{DH,low}$ compensating for the circulation heat loss to a slightly higher

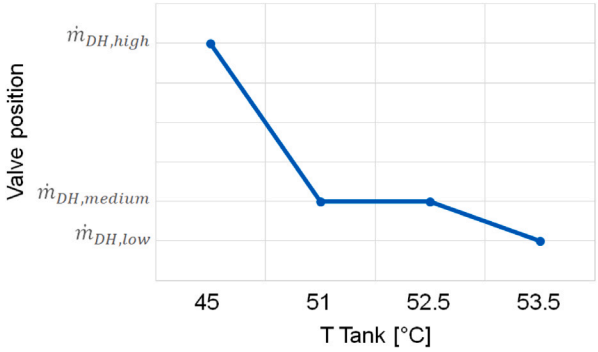

Fig. 4. Flow dictated by the primary valve according to the strategy based on a staged proportional controller.

flow represented by $\dot{m}_{DH,medium}$ meeting low DHW consumption. In line with the measurements, Eq. (9) and Eq. (10) can be used to calculate both flow rates.

$$\dot{m}_{DH,low} = \frac{P_{circ}}{c_w \cdot (T_{DH,sup} - 50)} \tag{9}$$

$$\dot{m}_{DH,medium} = \frac{P_{circ} + P_{55-54}}{c_w \cdot (T_{DH,sup} - 50)} \tag{10}$$

where P_{55-54} is the additional power supplied from the primary side when the DHW supply temperature reaches the level of 54 °C.

Otherwise, upon periods with remarkable use of DHW, the temperature measured by T_{Tank} may fall below 51 °C in which case the algorithm will activate the high-power control. In the unique case where this temperature drops to the critical temperature of 45 °C, the maximum flow rate $\dot{m}_{DH,high}$ shall be delivered. This can be estimated as shown in Eq. (11),

$$\dot{m}_{DH,high} = \frac{P_{circ} + P_{DHW,max}}{c_w \cdot (T_{DH,sup} - T_{DH,ret})} \tag{11}$$

with $P_{DHW,max}$ as the highest use of DHW.

2.2. Case study

The case under investigation is an existing multi-story building located in Hillerød, Denmark, where DH supplies the SH and DHW systems. It has 30 apartments, and the system for DHW preparation

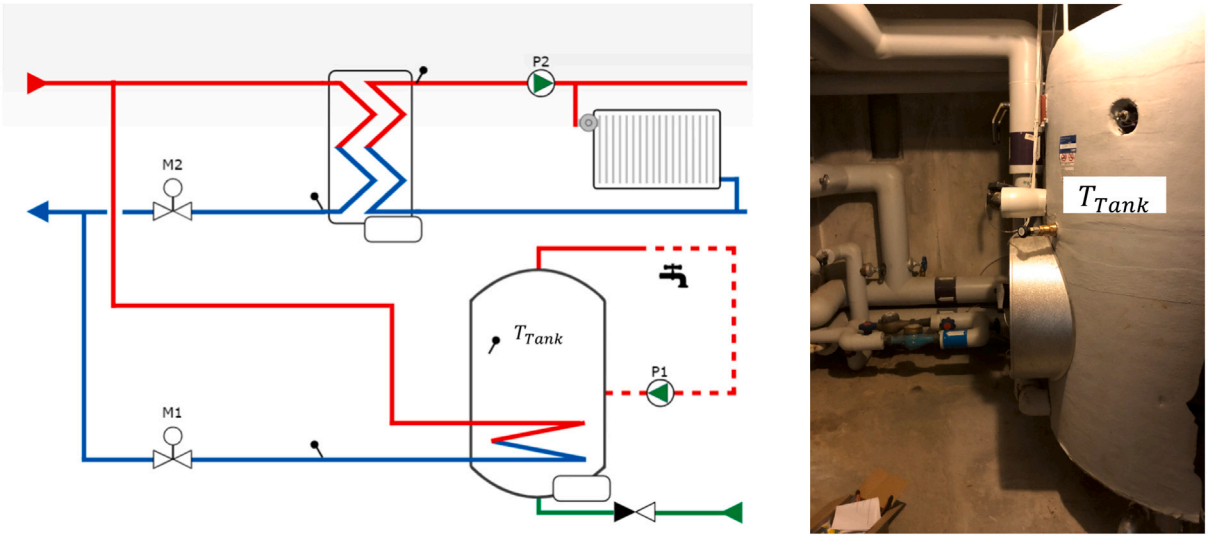

(a) Connection within the DH substation [25]. (b) DHW tank in the case study.

Fig. 5. DHW system configuration in the case study in Hillerød, Denmark. (see Ref. [25]).

consists of a typical storage tank with an internal heating coil and a circulation loop, as depicted in Fig. 5, with a nominal capacity of 1250 L. The substation in the basement incorporates the energy meters, enabling the application of the algorithms from the methods section. On the primary side, the data comprises the accumulated DH heat supplied to the DHW tank, the supply/return temperatures, and the DH flow rate. The secondary side meter reads the flow and temperature of the cold water entering the tank and the DHW supply temperature, which combines to provide the heating of tapped DHW. Given a typical set-point of 54 °C for the tank temperature (T_{Tank}) shown in Fig. 5, the conventional thermostatic control regulates the flow through the coil with no limit to the charging power.

2.2.1. Modeling approach

The development of a detailed dynamic model is essential to simulate and assess the performance of the new control concept. For this purpose, the study uses the Modelica Buildings Library [26] from Lawrence Berkeley National Laboratory. This open-source library has been extensively employed in recent research [27,28] and includes different components for buildings, district energy, and control systems. Plus, it is fairly flexible when it comes to modifying its items and thus leads to relatively fast modeling of existing buildings. This work uses a version of the tank model with an internal heating coil and a circulation loop for the simulations. Moreover, the use of the simulation environment Dymola made it possible to handle the Modelica [29] equations with ease.

Besides using a 14-day (336 h) dataset for system dimensioning, the performance evaluation used extended period measurements over the year 2021. The dynamic model employed the actual data of the DH supply temperature, cold water temperature, and tapping profile, all measured with a 20-second step resolution and used as inputs. Fig. 6 shows the supply/return temperature on the primary side of the tank and the DHW consumption profile. There is practically no DHW demand during the night, which leads to higher return temperatures. However, consumption peaks occur during the mornings and evenings. 30% of the time steps do not include any draw-off, and the peak demand is often 50–60 kW. The average power estimated for circulation heat losses is approximately 2.6 kW. Regardless of the time of the year, its value is nearly constant as represented in Fig. 7. This investigation assumed a cooling of 5 °C in the circulation loop, which has an estimated length of 115 m in the selected building.

The actual heat exchanger has a heating capacity (Q) of 92 kW with supply ($T_{primary,sup}$) and return ($T_{primary,ret}$) temperatures of 65/35 °C on the primary side, respectively, and supply ($T_{secondary,sup}$) and return ($T_{secondary,ret}$) temperatures of 10/50 °C on the secondary side, respectively. Thereby, the heat transfer coefficient (UA) is 4.7 kW/K according to Eq. (12)- Eq. (14).

$$Q = UA\frac{(\Delta T_2 - \Delta T_1)}{ln(\frac{\Delta T_2}{\Delta T_1})} \tag{12}$$

$$\Delta T_1 = T_{primary,sup} - T_{secondary,ret} \tag{13}$$

$$\Delta T_2 = T_{primary,ret} - T_{secondary,sup} \tag{14}$$

The authors divided the volume of the tank model into 40 layers, where layer 1 is the uppermost layer. Layers 12 and 36 hold the input and output of the heating coil, respectively. Considering that the circulation flow returns to the tank at layer 16, the circulation loop only uses 17% of the coil to compensate for its heat losses. For the case study, with a circulation heat loss of 2.6 kW, primary supply temperature of 66.4 °C, and secondary temperatures of 50/55 °C, the primary return temperature turns out to be 50.4 °C based on Eq. (12)- Eq. (14). Nevertheless, to simplify the algorithms, this study assumed that the primary flow cools down to 50 °C when heating the circulation loop.

The authors conducted an exhaustive validation of the model to confirm its accuracy and simulated the new charging concepts to evaluate their performance. A subsequent field implementation evinced the actual benefits of the staged control.

2.2.2. Field implementation

In the case study, a cloud-based SCADA solution enables remote control of the electronic controller (ECL). The authors executed the field tests by setting up a feedback loop with communication every 5 minutes between a remote computer and the ECL. In this way, the virtual controller prescribes the flows directly in the field according to the actual temperatures T_{DHW} and T_{Tank}. The valve position operates in a range of 0–10 V, with a resolution of 10 mV when running with the conventional control. However, the staged control modulates the valve position in steps of 0.1 V, since in the reference case, we can only prescribe the flows indirectly with the minimum and maximum valve positions. In terms of flow rate, this valve resolution translates into a step of $5.26 \cdot 10^{-3}$ kg/s.

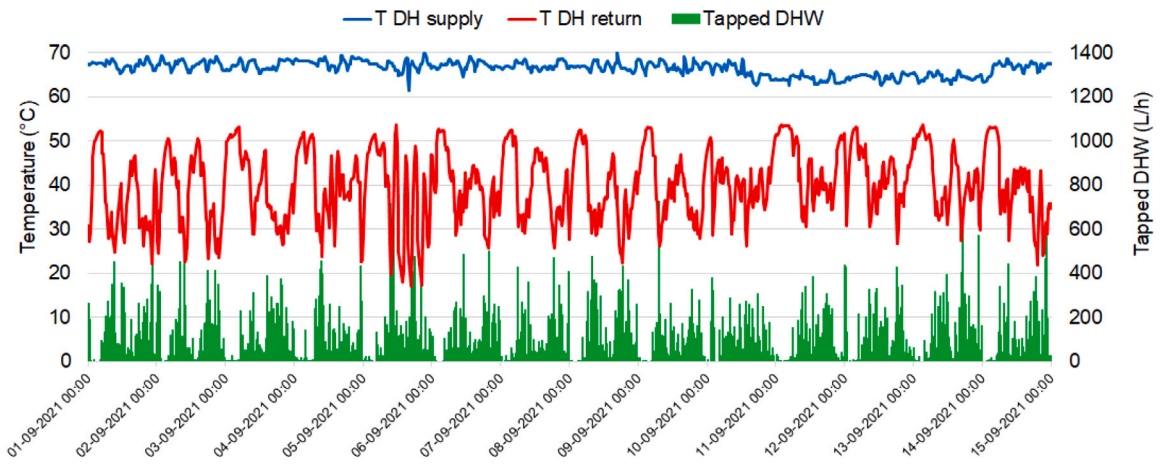

Fig. 6. DH supply/return temperatures of the DHW system and the 14-day consumption profile in the case study.

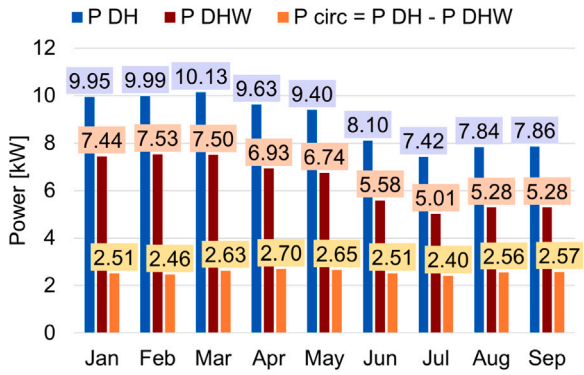

Fig. 7. The charging DH power, DHW demand and circulation loss in the case study before new strategy implementation.

Before implementing the new staged control, the authors refined its shaping parameters ($\dot{m}_{DH,low}$, $\dot{m}_{DH,medium}$, $\dot{m}_{DH,high}$) using the validated Modelica model. The authors subsequently conducted sensitivity analyses through simulations to assess the robustness of the concept to relaxed settings of the valve constraints, determining the influence of the parameters in the observed performance.

3. Results

This section firstly presents the Modelica model validation and secondly the simulation-based performance analyses of the new algorithms, employing actual data from the investigated building. Finally, after field implementation, the section exhibits comparative analyses between the conventional control and the new staged control. This comparison accounts for potential factors influencing the return temperature, such as the relative circulation loss.

3.1. Model validation

Attesting the tank model's accuracy, Fig. 8 depicts the DHW supply temperature and the DH return temperature, measured and simulated during five days. This period derives from the 14-day data used for model creation, shown in Fig. 6. The dynamic model used actual data as input for a fair comparison. Hence, the simulations employed the DH charging flow, the DHW tapping profile, the DH supply temperature and the cold water temperature provided from the field with a 20-seconds resolution. Both the DH return temperature and the DHW temperature represented in Fig. 8 confirm that the modelled storage

Table 1
Validation of modeled DHW installation. Comparison among simulated and measured data in the case study.

	Simulated	Measured
DHW temperature [°C]	56.6	56.3
DH return temperature [°C]	40.1	40.6
Heat loss coefficient [kW/K]	0.075	0.072

tank captures reality to the desired extent. To conduct a fair and simple evaluation of the return temperature of the system, Eq. (15) presents the calculation of the energy-weighted DH return temperature,

$$T_{DH,ret} = \frac{\int (E_{DH} \cdot T_{DH,ret\,ins})}{\int E_{DH}} \tag{15}$$

where E_{DH} represents the amount of heat energy delivered by the DH flow and $T_{DH,ret\,ins}$ is the DH return temperature of this flow. In particular, the energy-weighted DH return temperature is 40.1 °C in the model compared to 40.6 °C measured, and the average DHW temperature achieves the level of 56.6 °C in the model in contrast with the measured 56.3 °C. The simulated heat loss through the distribution pipes is also crucial for model validation. Thus, we calculate the heat loss coefficient as the ratio between the circulation heat losses and the temperature difference between the hot water inside the pipe and its envelope. These calculations assume a temperature of 20 °C for the riser system room. Table 1 summarizes the data used for the analysis.

The model also respects the buoyancy in the 40 layers of the tank. Thus, the layers above the circulation return, i.e. layer 16, remain close in temperature, and the profile of layer 40 is very similar to that of cold water temperature.

3.2. Simulation of modeled charging concepts

The operation of the concept based on energy balance is simple to illustrate with Fig. 9. According to the secondary side meter readings, the occupants in the reference building rarely consume DHW at night, yet the circulation heat losses require at least a low DH flow. Consequently, the tank bottom can accumulate up to 30kWh during the night. In instances with DHW use above the threshold, e.g. during morning and evening, the concept shaves the peak load by utilizing the stored heat in the tank bottom (E_{stored}). By the end of each day, the tank will have utilized almost all the stored heat. Thereby, this principle will enhance the temperature gradient in the tank ahead of periods with low draw-off. The power for DHW use has a step resolution of 3 kW at 20-minutes intervals. The threshold ($P_{DHW,threshold}$) for the use of DHW is slightly above 6 kW if calculated with an assumed target of 25 °C for the return temperature (Eq. (7)). In this way, the concept

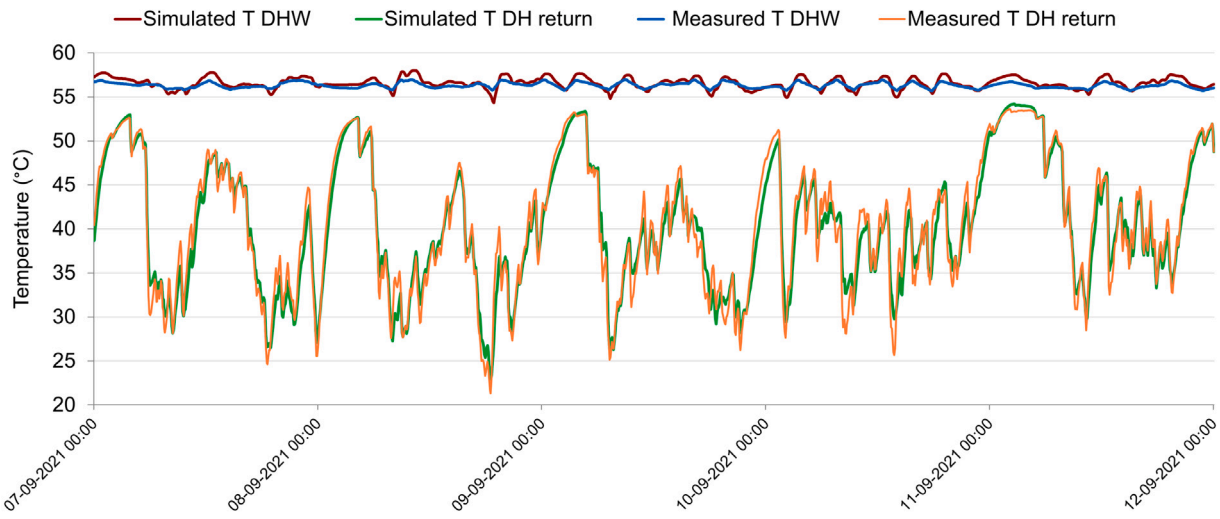

Fig. 8. Comparison of DHW Temperature and DH return temperature from simulations and actual data.

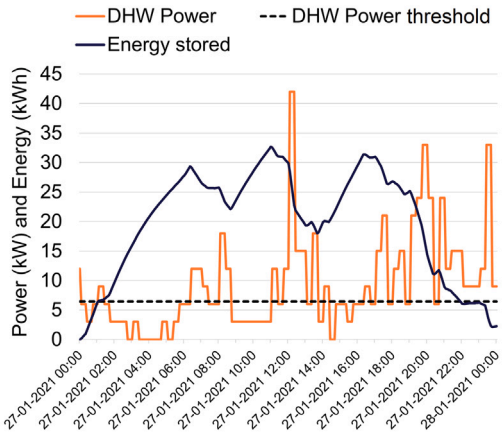

Fig. 9. Simulation of the accumulated energy inside the tank with the energy balance control.

supplies low DH flow if users consume 6 kW or less of DHW. For smoother charging operation and to prevent unnecessary fluctuations, the 20-minutes interval is assumed appropriate. Moreover, it allows a sufficient response margin in case of a sudden peak of DHW demand.

Fig. 10 shows the performance of both algorithms under an actual 10-day DHW tapping profile of the investigated case. The analysis focuses on the DHW supply temperature, the DH return temperature, and the DH supplied to the tank for comparison.

The energy balance control (Fig. 10(a)) secures a DHW temperature between 50 °C and 55 °C on days with moderate demand, such as December 1st. More specifically, it remains close to 55 °C, except in days with considerable tapping during the morning and evening periods, e.g. November 28th. The low DH flow rate ($\dot{m}_{DH,low}$) is sufficient to cover the circulation in low-tapping periods, heating the tank with just under 5 kW at night. Under high-tapping conditions, the heating coil has sufficient capacity to bring the DHW flow back to 55 °C and can deliver up to 35 kW at peak demand. Under this control algorithm, the simulated energy-weighted DH return temperature is 29 °C.

Simulation of the staged proportional controller reveals broadly similar performance to that of the energy balance control, as shown in Fig. 10(b). At low-tapping periods, e.g. at night, the control principle triggers the low-power stage, and the heat input can go below 5 kW.

Table 2
Charging flow rates needed for the staged control strategy.

Parameters	
$\dot{m}_{DH,low}$ [L/h]	136.5
$\dot{m}_{DH,medium}$ [L/h]	210.1
$\dot{m}_{DH,high}$ [L/h]	928.1

When the DHW temperature drops significantly due to high tapping, e.g. during November 30th in the evening, the heating coil delivers up to 55 kW within the high-power stage. Essentially, the minimum needed DH flow rates meet the safety requirements and even in situations with extraordinary demand, the concept secures the DHW supply temperature of 50 °C. With the staged control, the return temperature resulted in 28.8 °C. Table 2 presents the valve constraints required for the staged control applied herein. Hence, a $\dot{m}_{DH,low}$ of 136.5 L/h is sufficient to cover the 2.6 kW for circulation while maintaining the DHW supply temperature at 55 °C. The $\dot{m}_{DH,medium}$ of 210.1 L/h heats the circulation loop with 4 kW whenever the supplied DHW temperature drops to 54 °C. Finally, if the temperature at layer 14 (T_{Tank}) reaches the critical temperature of 45 °C, then a DH flow of 928.1 L/h would deliver approximately 50 kW.

The staged control simplifies the complexity and reinforces the strengths of the energy balance principle, with similar performance. However, the energy balance principle charges the tank every 20-minutes, whereas the staged control does so every 5 min. As a result, the DHW temperature drops during high-tapping periods are more conspicuous with the first strategy.

3.3. Field tests and sensitivity investigations

This section presents the field tests performed in the residential building in Hillerød. Fig. 11 depicts the actual tank operation with the newly implemented control. The strategy maintains the DHW temperature at 55 °C most of the time, except in periods with peak demand, where it guarantees a minimum of 50 °C through the activation of the control's peak-load stage. This operation observed in the field is notably similar to the simulations shown in Fig. 10(b), where the model employs an identical tapping profile. The return temperature measured after applying the new control is 29.7 °C, which also validates the control valve model.

In the investigated building, the conventional and the staged control were alternately implemented for three months achieving a 45-day

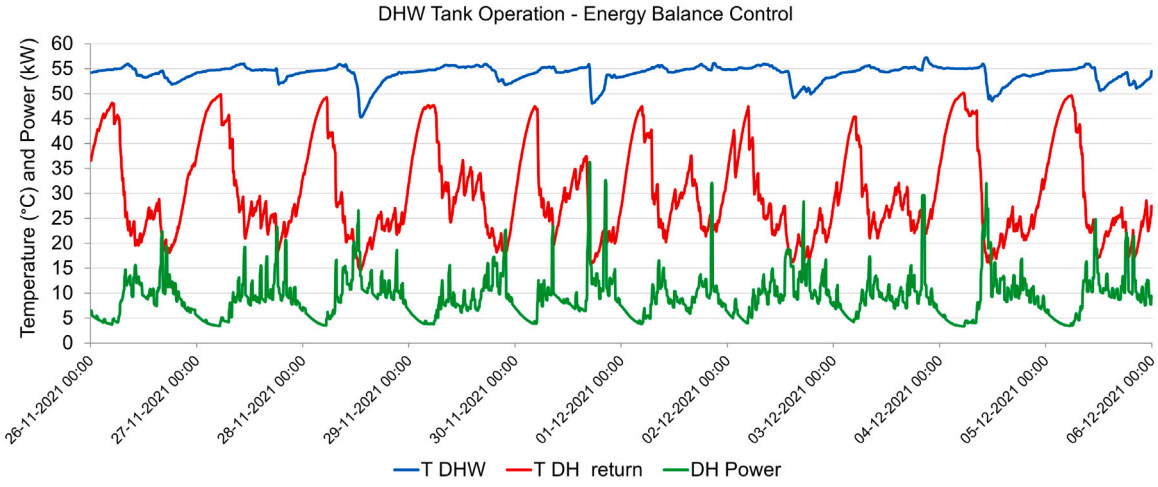

(a) DHW supply temperature, DH return temperature and DH power supplied to the tank with the energy balance control.

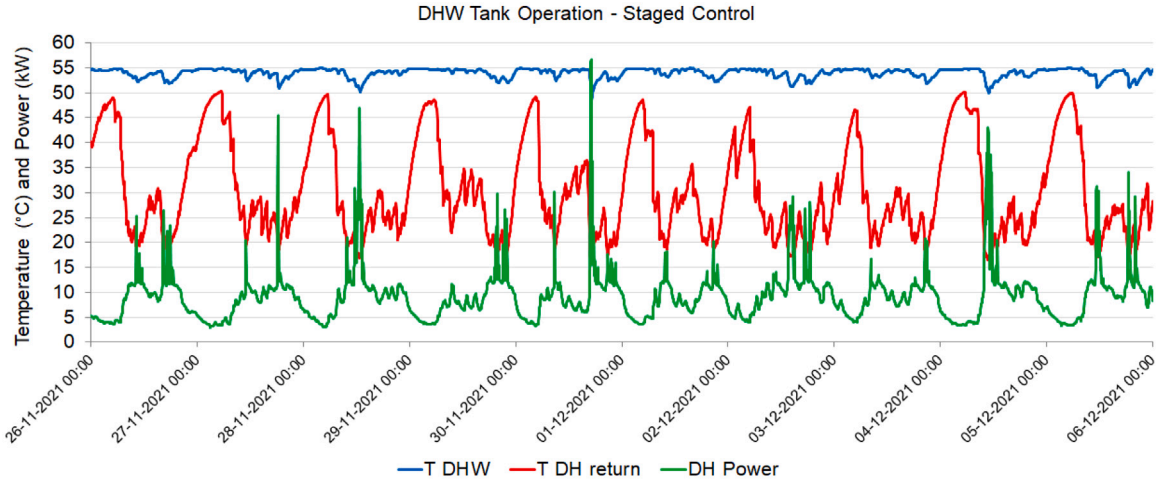

(b) DHW supply temperature, DH return temperature and DH power supplied to the tank with the staged control.

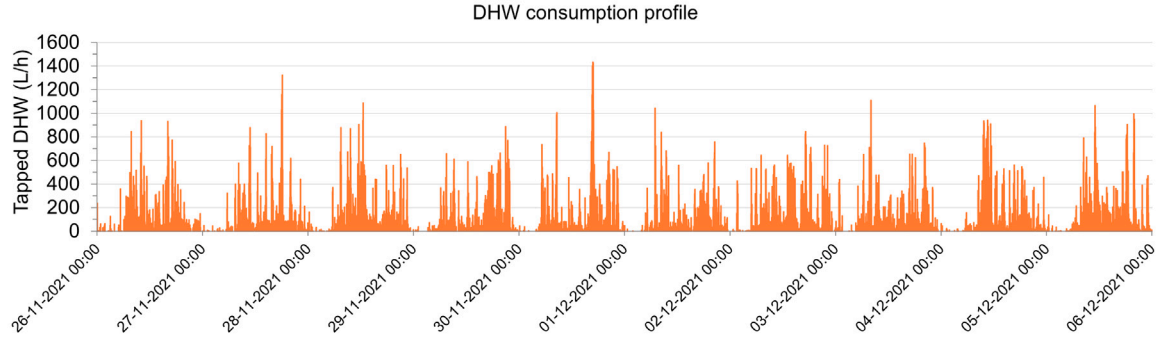

(c) Actual 10-days DHW consumption profile in the case study.

Fig. 10. Comparison between the simulated energy balance control and staged control.

dataset for each strategy. The analysis of the measured return temperature accounted for the variation in relative circulation heat losses (P_{circ}/P_{DHW}), DHW supply temperature, DH supply temperature, and cold-water temperature. Fig. 12 shows the measured return temperature with these four factors. Firstly, the higher hot water utilization – i.e. when P_{circ}/P_{DHW} is low – resulted in lower return temperature for both strategies. Secondly, the staged control supplies DHW between 54.5 °C and 55.5 °C on average, and the conventional control shows a higher return temperature for the same temperature range. In both situations, the supply temperature set-points are comparable at low draw-off periods. The graph shows that, at equal DH supply temperature, the return temperature is usually higher with the conventional control. Finally, the last scatter plot reveals that the domestic cold water temperature plays a relevant role in the return temperature. Even at equal cold water temperature, the staged control performs better. From this graph, it is also possible to deduce the cold-water temperature variation in the case study from September 2021 to early January 2022.

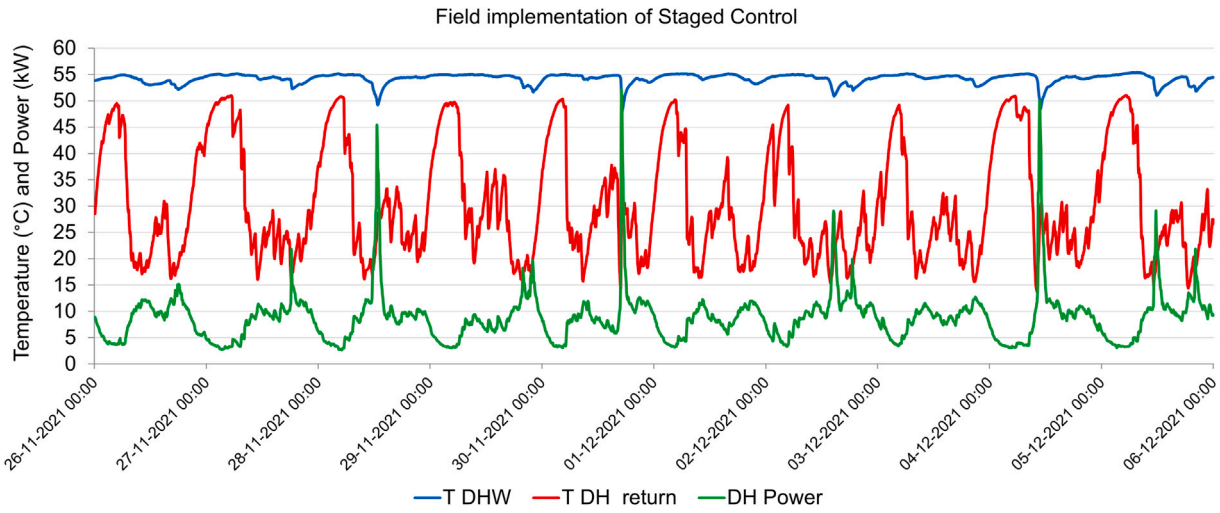

Fig. 11. Actual DHW supply temperature, DH return temperature, and DH power supplied to the tank with the new staged control.

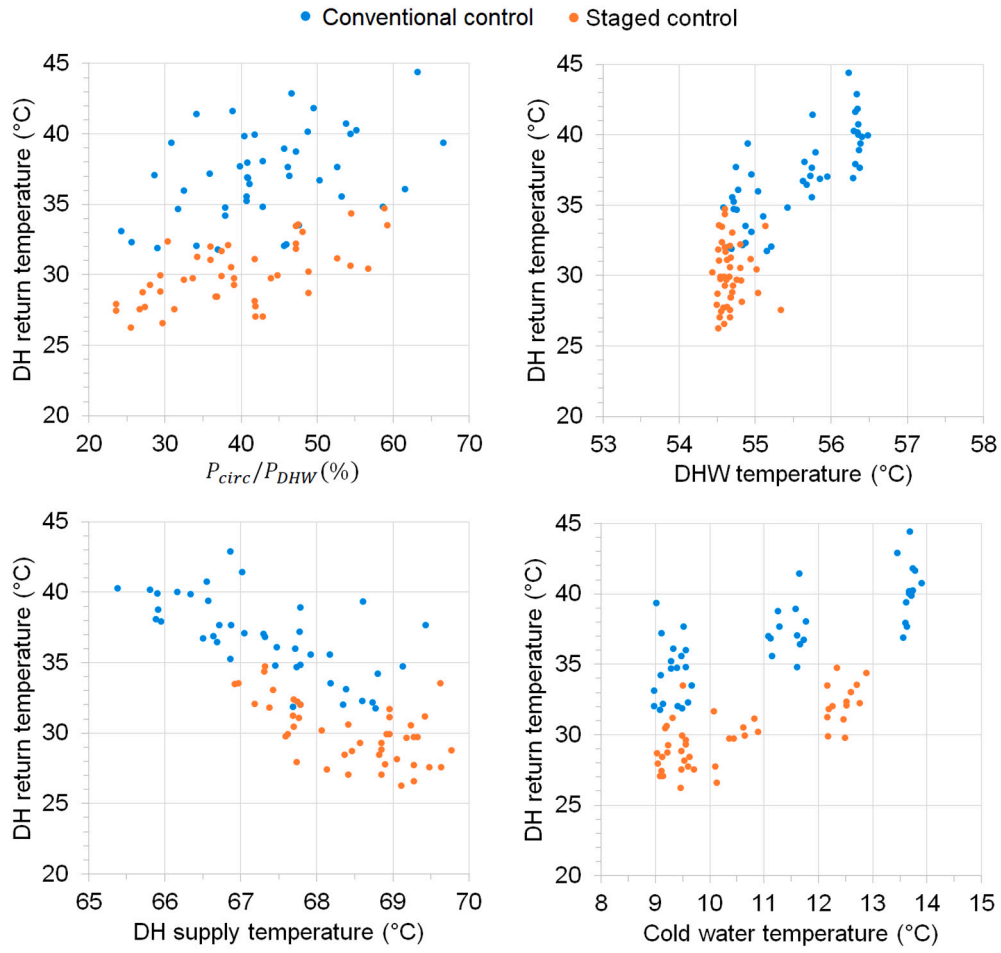

Fig. 12. Comparative analysis among normal and new staged control with measured data in Hillerød, Denmark.

Fig. 13 shows the daily energy-weighted DH return temperatures achieved with each strategy. The data gathered during 90 days of field tests populated this statistical analysis. A clear reduction in return temperature is realized from 37.0 °C to 30.0 °C, due to new control concept application.

A well-functioning primary valve should operate at moderate valve positions most of the time, thus avoiding harming the DH operation with unnecessary excessive flows when securing the heating of the tank to the set-point quickly after a peak consumption. Fig. 14 shows the cumulative frequency of primary valve positions measured in each

Table 3
Influence of valve position constraints ($\dot{m}_{DH,low}$, $\dot{m}_{DH,medium}$, $\dot{m}_{DH,high}$) in the system performance with the staged control.

Parameters	$\dot{m}_{DH,low}$	VP_{low}	$\dot{m}_{DH,medium}$	VP_{medium}	$\dot{m}_{DH,high}$	VP_{high}	T_{DHW}	$T_{DH,ret}$
Implementation set	136.5 L/h	1.4 V	210.1 L/h	1.8 V	928.1 L/h	5.6 V	54.6 °C	28.8 °C
Scenario 1	136.5 L/h	1.4 V	210.1 L/h	1.8 V	**1769.4** L/h	**10.0 V**	54.6 °C	28.8 °C
Scenario 2	136.5 L/h	1.4 V	**320.3 L/h**	**2.3 V**	928.1 L/h	5.6 V	54.8 °C	29.4 °C
Scenario 3	**0.0 L/h**	**0.7 V**	210.1 L/h	1.8 V	928.1 L/h	5.6 V	54.3 °C	28.3 °C

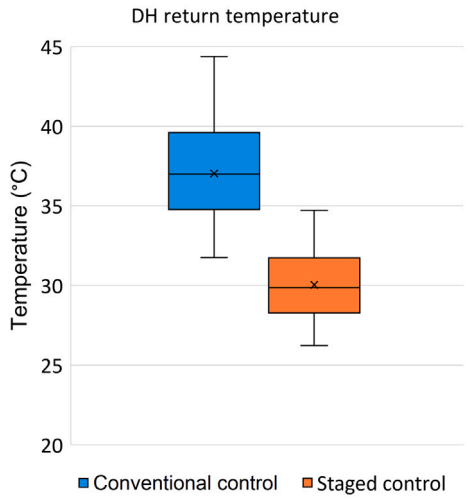

Fig. 13. Comparison between normal and staged control by statistical analysis of the energy-weighted DH return temperatures measured in Hillerød, Denmark.

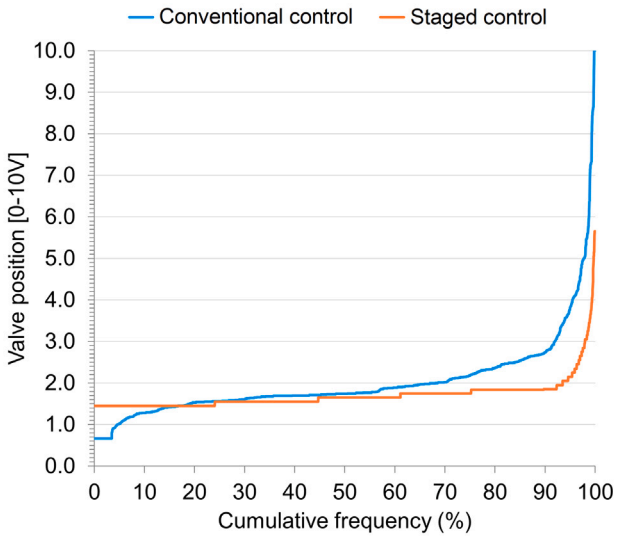

Fig. 14. Comparison among strategies through cumulative curves of measured valve positions for charging the DHW tank from DH.

strategy during 10 days. The conventional control operates over a broader range of valve positions than the staged control, as it opens and closes fully. The staged control works to a greater extent at the low DH flow stage (1.4–1.8 V). Furthermore, the staged control cannot open more than the designed maximum position (VP_{high}), which is 5.6 V. It must also guarantee the minimum flow to cover the circulation heat loss and does not close fully at any time. In particular, the accumulated DH flow used for the conventional control is 62.4 m^3 in 10 days, whereas in the staged control is 47.7 m^3 , which means savings of 23.6% in the total DH volume.

Finally, the new staged control concept should be robust to relaxed settings of the valve constraints, thus demonstrating minimal configuration requirements for new implementations. In this way, the influence of these parameters on the observed performance will be minimal. Table 3 determines how the valve constraints affect DHW supply temperature (T_{DHW}) and DH return temperature ($T_{DH,ret}$) when applying the staged control. By simulating the system for the same period as in Fig. 10(b), the first scenario points out that increasing $\dot{m}_{DH,high}$ does not influence the system performance. Since this flow is rarely needed, the maximum valve position of 5.6 V is sufficient. An increase of 0.5 V in VP_{medium} (Scenario 2) does not lead to large deviations in return temperature either. In this case, return temperature rises by 0.6 °C, but so does DHW supply temperature, albeit to a lesser extent. Similarly, when $\dot{m}_{DH,low}$ becomes 0.0 L/h (Scenario 3), the return temperature decreases moderately at the cost of a lower DHW supply temperature.

4. Discussion

A new staged control concept revealed encouraging results for DH return temperatures reduction in DHW storage tanks with an internal heating coil and a circulation loop. The tested algorithm supplies the minimum DH flow to compensate for circulation heat losses and DHW consumption, which resulted in a 7 °C reduction of DH return temperature (Fig. 13). According to Fig. 11, this also secured a tank operation with DHW supply temperature in line with regulations, thus complying with hygienic and comfort conditions. Compared to the conventional control, the staged control frequently operates at more moderate valve positions (Fig. 14). The suggested concept saves 23.6% in DH flow and avoids unnecessary load fluctuations so as not to harm the cooling of the tank bottom. In addition, the principle is relatively straightforward to implement and does not need additional investment, as only the existing electronic controller shall be adjusted. In the reference building, a pressure-independent valve and an extra sensor at the tank outlet made the implementation much simpler when prescribing the flows, where the measured performance (Fig. 11) was in line with the simulations (Fig. 10(b)).

The non-uniformity of the DHW consumption profile is still a limiting factor for the reduction of return temperatures in DHW tanks with a circulation loop, even with the improved control concept. According to Figs. 9–11, the heating of the bottom-half part of the tank still occurs due to the continuous compensation of circulation losses, not only at night but also during the daytime. As a result, the return temperature can increase towards 50 °C. However, we can observe return temperatures below 20 °C in periods with high hot water utilization, e.g. in the morning or evening. Similarly, as stated in Fig. 12, in both the conventional control and staged control concepts, higher relative circulation losses lead to higher return temperatures. Thus, we can achieve return temperatures around 25 °C on days with high draw-off when applying the staged control.

Boundary conditions, such as cold water temperature and DH supply temperature, also influence the measured return temperature (Fig. 12). Therefore, the evaluation of the tank performance must consider the seasonality of both boundary conditions and the DHW tapping (Fig. 7), as the potentially achievable return temperature may differ from season to season.

In the case study, the DH supply temperature can vary between 65–70 °C and the relative circulation heat loss (P_{circ}/P_{DHW}) ranges

between 20–70% (Fig. 12). Nevertheless, the situation may be different in other buildings, either with higher circulation losses (e.g. in non-refurbished or non-residential buildings) or where a lower temperature DH network supplies the system. In both situations, the flow through the heating coil to cover the circulation might be too large. Thus, there would be no opportunity to reduce the return temperatures by only improving the control concept. Likewise, the return temperatures turned out to be higher on those days with relatively low use of DHW.

5. Conclusion

This paper presents the development of two new control concepts to reduce the return temperatures in DHW tanks with a circulation loop. The authors built and validated a dynamic model with measured data from a residential building in Hillerød, Denmark, and investigated the performance of the control concepts with actual DHW tapping profiles. Finally, the authors tested the simplified control strategy — known as staged control — in the field and compared the resulting operation to a reference conventional control. The conclusions inferred from the analysis of the new charging control confirm that:

- The implementation of the new charging concept resulted in 7 °C lower DH return temperatures on average and DH flow savings of 23.6%.
- Staged control achieved DH return temperatures below 30 °C, and hygienic standards for DHW preparation are always satisfied without the need for further investment.
- The existence of circulation through the tank limits the possibility of further return temperature reduction. The staged control achieved DH return temperatures around 25 °C on days with high draw-off.
- The seasonality of both boundary conditions and DHW demand influences the potential for lower return temperatures.
- A detailed dynamic model of the system has considerably reduced testing times, and simulations have accurately represented the actual measurements.

In future research, the dynamic model can be used to calculate the optimal trajectory of DH flow, giving an indicator of the minimum achievable DH return temperature in DHW tanks. In addition, the model can be used to investigate the feasibility of new DHW system configurations to limit the negative impact of circulation on return temperatures.

CRediT authorship contribution statement

Abdelkarim Tahiri: Conceptualization, Methodology, Software, Investigation, Writing – original draft, Visualization. **Kevin Michael Smith:** Conceptualization, Methodology, Writing – review & editing, Supervision. **Jan Eric Thorsen:** Investigation. **Christian Anker Hviid:** Supervision. **Svend Svendsen:** Conceptualization, Methodology, Supervision.

Declaration of competing interest

The authors declare that they have no known competing financial interests or personal relationships that could have appeared to influence the work reported in this paper.

Data availability

Data will be made available on request.

Acknowledgment

The Danish Innovation Fund, Denmark funded this work as part of the HEAT 4.0 project (grant number 8090-00046B). The authors gratefully acknowledge the collaboration provided by the HEAT 4.0 project and would like to thank Danfoss for their support and for sharing the data to conduct the study.

References

[1] Commission E. 2030 Climate target plan. 2022, https://ec.europa.eu/clima/eu-action/european-green-deal/2030-climate-target-plan_en, [Accessed: 2022-02-09].
[2] Lund H, Werner S, Wiltshire R, Svendsen S, Thorsen JE, Hvelplund F, et al. 4th Generation District Heating (4GDH): Integrating smart thermal grids into future sustainable energy systems. Energy 2014;68:1–11. http://dx.doi.org/10.1016/j.energy.2014.02.089, https://www.sciencedirect.com/science/article/pii/S0360544214002369.
[3] Connolly D, Lund H, Mathiesen B, Werner S, Möller B, Persson U, et al. Heat Roadmap Europe: Combining district heating with heat savings to decarbonise the EU energy system. Energy Policy 2014;65:475–89. http://dx.doi.org/10.1016/j.enpol.2013.10.035, https://www.sciencedirect.com/science/article/pii/S0301421513010574.
[4] Lund H, Østergaard PA, Chang M, Werner S, Svendsen S, Sorknæs P, et al. The status of 4th generation district heating: Research and results. Energy 2018;164:147–59. http://dx.doi.org/10.1016/j.energy.2018.08.206, https://www.sciencedirect.com/science/article/pii/S0360544218317420.
[5] Agency DE. Danish experiences on district heating. 2019, https://ens.dk/en/our-responsibilities/global-cooperation/experiences-district-heating, [Accessed: 2022-02-09].
[6] Marszal-Pomianowska A, Zhang C, Pomianowski M, Heiselberg P, Gram-Hanssen K, Rhiger Hansen A. Simple methodology to estimate the mean hourly and the daily profiles of domestic hot water demand from hourly total heating readings. Energy Build 2019;184:53–64. http://dx.doi.org/10.1016/j.enbuild.2018.11.035, https://www.sciencedirect.com/science/article/pii/S0378778818321261.
[7] Bøhm B. Production and distribution of domestic hot water in selected danish apartment buildings and institutions. Analysis of consumption, energy efficiency and the significance for energy design requirements of buildings. Energy Convers Manage 2013;67:152–9. http://dx.doi.org/10.1016/j.enconman.2012.11.002, https://www.sciencedirect.com/science/article/pii/S0196890412004384.
[8] Pomianowski M, Johra H, Marszal-Pomianowska A, Zhang C. Sustainable and energy-efficient domestic hot water systems: A review. Renew Sustain Energy Rev 2020;128:109900. http://dx.doi.org/10.1016/j.rser.2020.109900, https://www.sciencedirect.com/science/article/pii/S1364032120301921.
[9] Ivanko D, Walnum HT, Nord N. Development and analysis of hourly DHW heat use profiles in nursing homes in Norway. Energy Build 2020;222:110070. http://dx.doi.org/10.1016/j.enbuild.2020.110070, https://www.sciencedirect.com/science/article/pii/S0378778819336126.
[10] Lidberg T, Olofsson T, Ödlund L. Impact of domestic hot water systems on district heating temperatures. Energies 2019;12(24). http://dx.doi.org/10.3390/en12244694, https://www.mdpi.com/1996-1073/12/24/4694.
[11] Standards D. DS 439:2009-norm for vandinstallationer [code of practice for domesticwater supply]. 2009, [In Danish] https://webshop.ds.dk/en-gb/standard/ds-4392009?CurrencyCode=EUR, [Accessed: 2022-02-14].
[12] Standards D. DS 469:2013-heating and cooling systems in buildings. 2013, https://webshop.ds.dk/en-gb/standard/ds-4692013, [Accessed: 2022-02-14].
[13] Benakopoulos T, Vergo W, Tunzi M, Salenbien R, Svendsen S. Overview of solutions for the low-temperature operation of domestic hot-water systems with a circulation loop. Energies 2021;14(11). http://dx.doi.org/10.3390/en14113350, https://www.mdpi.com/1996-1073/14/11/3350.
[14] Maltais L-G, Gosselin L. Predictability analysis of domestic hot water consumption with neural networks: From single units to large residential buildings. Energy 2021;229:120658. http://dx.doi.org/10.1016/j.energy.2021.120658, https://www.sciencedirect.com/science/article/pii/S0360544221009075.
[15] Sborz J, Cominato C, Kalbusch A, Henning E. Hourly and daily domestic hot water consumption in social housing dwellings: An analysis in apartment buildings in Southern Brazil. Sol Energy 2022;232:459–70. http://dx.doi.org/10.1016/j.solener.2021.12.067, https://www.sciencedirect.com/science/article/pii/S0038092X21011166.
[16] Fuentes E, Arce L, Salom J. A review of domestic hot water consumption profiles for application in systems and buildings energy performance analysis. Renew Sustain Energy Rev 2018;81:1530–47. http://dx.doi.org/10.1016/j.rser.2017.05.229, https://www.sciencedirect.com/science/article/pii/S1364032117308614.
[17] Averfalk H, Möllerström E, Ottermo F. Domestic hot water design and flow measurements. The 17th International Symposium on District Heating and Cooling, Energy Rep 2021;7:304–10. http://dx.doi.org/10.1016/j.egyr.2021.08.142, https://www.sciencedirect.com/science/article/pii/S2352484721007459.

[18] Yang L, Bøhm B, Paulsen O, Frederiksen S. Evaluation of the dynamic performance of a hot water tank with built-in heating coil. Int J Energy Res 1997;21(3):265–74.
[19] Thorsen JE, Skov M, Honoré K. Installation and demonstration of domestic hot water circulation booster for reducing district heating return temperature Deliverable No: D5.4b. 2019, http://www.energylabnordhavn.com/uploads/3/9/5/5/39555879/d5.4b_dhw_circulation_booster.pdf, [Accessed: 2022-02-15].
[20] Yang X, Svendsen S. Ultra-low temperature district heating system with central heat pump and local boosters for low-heat-density area: Analyses on a real case in Denmark. Energy 2018;159:243–51. http://dx.doi.org/10.1016/j.energy.2018.06.068, https://www.sciencedirect.com/science/article/pii/S0360544218311332.
[21] Hermansen R, Smith K, Thorsen JE, Wang J, Zong Y. Model predictive control for a heat booster substation in ultra low temperature district heating systems. Energy 2022;238:121631. http://dx.doi.org/10.1016/j.energy.2021.121631, https://www.sciencedirect.com/science/article/pii/S036054422101879X.
[22] Yang X, Honoré K. Installation and demonstration of capacity limitation functionality for domestic hot water tank in a new building to reduce peak load, lower return temperature and utilize thermal flexibility in domestic hot water tanks Deliverable No: D5.4c (i). 2019, http://www.energylabnordhavn.com/uploads/3/9/5/5/39555879/d5.4c_i_optimum_dhw_new_building.pdf, [Accessed: 2022-02-15].
[23] Huang T, Yang X, Svendsen S. Multi-mode control method for the existing domestic hot water storage tanks with district heating supply. Energy 2020;191:116517. http://dx.doi.org/10.1016/j.energy.2019.116517, https://www.sciencedirect.com/science/article/pii/S0360544219322121.
[24] Yang X, Svendsen S. Improving the district heating operation by innovative layout and control strategy of the hot water storage tank. Energy Build 2020;224:110273. http://dx.doi.org/10.1016/j.enbuild.2020.110273, https://www.sciencedirect.com/science/article/pii/S0378778820306733.
[25] Danfoss. Cloud-based SCADA solution for ECL Comfort 296 / ECL Comfort 310 controllers. 2018, https://assets.danfoss.com/documents/75259/AI148886473107en-010501.pdf, [Accessed: 2022-03-15].
[26] Labs B. Modelica buildings library. 2020, https://simulationresearch.lbl.gov/modelica/, [Accessed: 2022-01-03].
[27] Abugabbara M, Lindhe J, Javed S, Bagge H, Johansson D. Modelica-based simulations of decentralised substations to support decarbonisation of district heating and cooling. The 17th International Symposium on District Heating and Cooling, Energy Rep 2021;7:465–72. http://dx.doi.org/10.1016/j.egyr.2021.08.081, https://www.sciencedirect.com/science/article/pii/S2352484721006831.
[28] Faulkner CA, Castellini JE, Zuo W, Lorenzetti DM, Sohn MD. Investigation of HVAC operation strategies for office buildings during COVID-19 pandemic. Build Environ 2022;207:108519. http://dx.doi.org/10.1016/j.buildenv.2021.108519, https://www.sciencedirect.com/science/article/pii/S0360132321009148.
[29] Association TM. Modelica language. 2021, https://modelica.org/modelicalanguage.html, [Accessed: 2022-01-03].